High-Pressure Viscosity of Dilute Polymer Solutions in Good Solvents

Richard L. Cook,† H. E. King, Jr.,* and Dennis G. Peiffer

Corporate Research Science Laboratories, Exxon Research and Engineering Company, Route 22 East, Clinton Township, Annandale, New Jersey 08801

Received December 26, 1991; Revised Manuscript Received January 31, 1992

ABSTRACT: The high-pressure viscosities of four dilute, good-solvent polymer solutions [polystyrene (PS) in tetrahydrofuran (THF) and chloroform, polyisobutylene (PIB) in THF, and partially hydrolyzed polyacrylamide (HPAM) in 2% NaCl-water] were measured in a new diamond-anvil cell viscometer at pressures up to 20 kbar. The viscosity of these polymer solutions rises faster with increasing pressure than the viscosity of the solvents in the absence of the polymers. The specific viscosity, η_{sp}, was calculated at high pressure by obtaining the ratio of solution to solvent viscosity at each pressure. The intrinsic viscosity, $[\eta]$, was then calculated using the well-known Huggins equation. After the concentration is corrected to reflect decreasing solvent volume as a result of compression at high pressure, η_{sp} plotted against concentration falls on a single curve at all pressures. This curve is identical to the curve determined at ambient pressure. Thus $[\eta]$ is pressure invariant to within our experimental uncertainty, 10%. The application of simple dilute polymer solution theory further implies that the radius of gyration is also invariant with pressure. The implication of this finding is that the increase in η_{sp} with pressure arises solely from the increased volume fraction of the polymer per unit volume of the solvent.

Introduction

Understanding the relationship between the structure of polymers and their viscosity is of fundamental importance in the study of polymers. An important quantification of this relationship is given by the dilute solution theory of Flory[1] which shows that the intrinsic viscosity, $[\eta]$, at a given molecular weight is dependent on the radius of gyration. The role of changes in temperature, solvent quality, concentration, chain architecture, and molecular weight upon both radius of gyration and $[\eta]$ has been explored by extensive theoretical efforts and many experimental studies.[2-6] Much less investigated is the role of pressure changes. Pressure being a basic thermodynamic parameter, one can expect that such studies can give insight into the fundamental interactions controlling solution behavior. For example, information on the relative importance of energetic and entropic terms in the variation of R_g can be extracted from high-pressure studies.[7,8] In addition, the response of polymer solution viscosity to high pressure can have important technical consequences. Polymers are frequently added as viscosifiers to enhanced oil recovery fluids where pressures of a couple thousand atmospheres are encountered.[9,10] It is known that during normal polymer processing, pressures up to several hundred atmospheres can be encountered in extrusion and even thousands of atmospheres in pressure molding; alteration of the polymer configuration under these pressures could have significant implications.[11,12] Finally, one of the highest pressure technical applications of polymer solutions is in lubrication, where fluid pressures can reach values up to 40 kbar.[13] Typical lubricants consist of a hydrocarbon solvent containing polymer additives at low concentration.

There have been a number of previous high-pressure studies on polymer solutions; typically these are made over a moderate pressure range ($P < 3.5$ kbar) and involve the measurement of the intrinsic viscosity, radius of gyration (R_g), hydrodynamic radius (R_h), or second virial coefficient (A_2). These quantities are interrelated; however, reports on the variation of these four quantities indicate no consistent trends in chain dimensions with increasing pressure. Measurements of viscosity uniformly show $[\eta]$ to increase with pressure (typically $\approx 20\%$ in 1 kbar).[14-25] This result implies that the other three aforementioned values should also increase with pressure. The radius of gyration, however, shows no consistent trend with pressure.[7,8,26-28] Measurements of polymers in good solvents show that R_g may either increase or decrease with increasing pressure. The range of variation is $\pm 15\%$/kbar. Θ solvents also exhibit an increasing or decreasing R_g, but the magnitude of the change may be as large as $\pm 25\%$/kbar. The variation of A_2 is from $\pm 5 \times 10^{-4}$ cm^3 mol g^{-2} kbar^{-1} for both good and Θ solvents, with most systems exhibiting a change of less than $\pm 5 \times 10^{-5}$ cm^3 mol g^{-2} kbar^{-1}.[7,8,26-30] For the good-solvent system, polystyrene in toluene, R_h is invariant with pressure.[31,32] In two other studies on macromolecular solutions, R_h was found to increase by about 15% in a 2-kbar range due to effects such as denaturation, aggregation, and degradation.[33,34] In order to gain an appreciation for the range of the available data, it is instructive to examine polystyrene in a good solvent (toluene), a system where all four quantities have been measured. Published results indicate that $[\eta]$ increases by 32% in 1 kbar,[21] R_g decreases by 12% in 0.75 kbar,[7] A_2 is nearly constant over 4 kbar,[7,30] and R_h is invariant in 5 kbar.[31,32]

As noted, the four quantities mentioned above are interrelated and one of the most straightforward relationships is between the intrinsic viscosity and radius of gyration as given by the dilute solution theory of Flory.[1]

$$[\eta] = \Phi' \langle s^2 \rangle^{3/2} M^{-1} \tag{1}$$

$\Phi' = 6^{3/2}\Phi \approx 3.7 \times 10^{22}$ dL mol^{-1} cm^{-3}, Φ = Flory constant, $\langle s^2 \rangle^{1/2}$ = radius of gyration, and M = molecular weight. (Note: Modern theory suggests that $\langle s^2 \rangle^{1/2}$ in eq 1 is equal to $R_g^{2/3} R_h^{1/3}$.[35] In the remainder of the text, we will use the phrase "radius of gyration" to represent $\langle s^2 \rangle^{1/2}$ in eq 1.) As $[\eta]$ increases with pressure for all of the literature data above, eq 1 states that the radius of gyration must also increase. This is clearly not the case. This inconsistency suggests a need for further high-pressure viscosity

† Current address: Department of Chemistry, Harvard University, Cambridge, MA 02138.

0024-9297/92/2225-2928$03.00/0

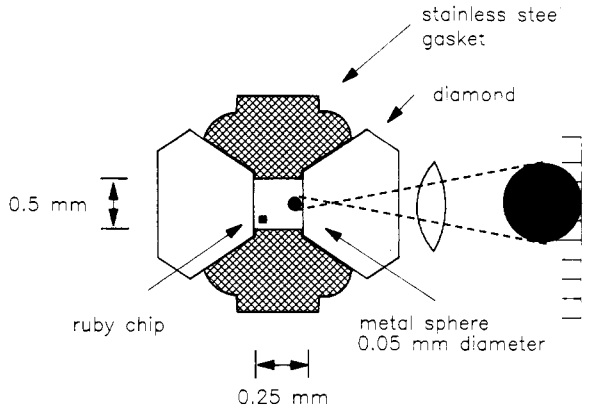

Figure 1. Schematic diagram of the diamond-anvil cell viscometer. The cell is rotated 180° about an axis normal to the diamond walls, and the ball rolls down the surface of the diamond under the force of gravity.

data and a reexamination of the calculations of $[\eta]$ from data in the literature.

In this work, the viscosity–pressure relationships in single-component dilute polymer solutions using good solvents are examined. High-pressure viscosities are reported, and the results are used to obtain $[\eta]$ as a function of pressure. There are two significant differences in our measurements from those published previously: (1) The pressure range has been extended (exceeding the previous published maximum of 3.5 kbar)[20,24] to the freezing point of the solutions, i.e., up to 20 kbar in tetrahydrofuran (THF), using a newly developed diamond-anvil cell viscometer.[36] (2) A concentration correction for the calculation of $[\eta]$ has been introduced that explains the scaling of η_{sp} with pressure. The resulting $[\eta]$ values are found to be pressure independent to within experimental accuracy for the four systems studied here. The implications of these findings with regard to polymer structure and radius of gyration are discussed.

Experimental Section

The viscosity measurements were made by recording the velocity of a falling ball inside a diamond-anvil cell. A full report describing this device has been published elsewhere,[36] and only a brief description is given here. The pressure chamber consists of a 500-μm-diameter hole drilled in a 250-μm-thick piece of stainless steel which is compressed between two flat diamond surfaces. The ball, a nickel alloy about 50 μm in diameter, rolls down the surface of one of the diamonds. A schematic of the diamond-anvil cell viscometer is given in Figure 1.

A video camera relays the image of the ball to a video dimension analyzer (VDA) which returns a voltage proportional to the displacement of the ball. A computer makes periodic readings of the VDA output, giving displacement as a function of time. The slope of the line thus obtained yields the velocity of the ball which can be converted into viscosity, η, by a modified Stokes equation

$$\eta = \gamma[2R^2g(\rho_s - \rho_f)\cos\theta]/9v \qquad (2)$$

where R = sphere radius, g = acceleration of gravity, ρ_s = sphere density (7.6 g/mL), ρ_f = fluid density, θ = tilt angle of cell (0° = vertical), v = velocity of the ball, and γ = wall correction. All of the above parameters are experimentally measurable, with γ being an instrument constant dependent only on the tilt angle. We determine γ for each experiment by taking the ratio of the observed ambient pressure velocity in the diamond cell to the Stokes velocity obtained from an independent measurement of the ambient-pressure viscosity in a Contraves low-shear 30 viscometer. Experiments have shown that γ defined in this manner is then pressure independent.[36]

The pressure in the diamond cell is measured by use of the ruby fluorescence peak, λ = 694.26 nm at ambient pressure, which shifts in frequency under pressure.[37] The measurements on the polymer solutions were in the 0–20-kbar range (1 kbar = 0.1 GPa ≅ 1000 atm), the upper pressure being limited only by the freezing pressure of the solvents (experimentally determined and reported in Table I). Pressure measurements are accurate to ±0.3 kbar.

The fluid density term ρ_f in eq 2 varies with pressure as the compressibility of the solvent. We calculate ρ_f from the Birch–Murnaghan equation of state[38] using compressibility data from the literature.[39-42] The compressibility of the polymer solutions can be approximated by the solvent compressibility at these dilute concentrations.

Viscosities determined by the diamond-anvil cell viscometer have a precision of ≈4%, and data taken on materials with known viscosity vs pressure behavior have established the accuracy of the measurements.[36] Viscosity measurements in the present experiment were taken in both increasing and decreasing pressure; in all cases the results are fully reversible and the ambient viscosity was recovered after the pressure was released. Because the $[\eta]$ calculations involve the ratio of two viscosities, the resulting $[\eta]$ values are accurate to ≈10%. All measurements were made at 22.5 ± 1 °C.

The molecular weights of the PS and PIB were 300 000 and 160 000, with polydispersities (M_w/M_n) of 1.06 and 1.08, respectively. The solvents were spectrophotometric grade and used as received. The partially hydrolyzed polyacrylamide (HPAM) was polydisperse with the following characteristics: M_w = 3 000 000, M_w/M_n = 1.42, and carboxylate content = 20 mol %. The solvent was a 2% NaCl solution in distilled water stabilized with 50 ppm formaldehyde. Solvent properties relevant to the high-pressure studies are outlined in Table I. In each case the dilute solutions were formulated such that at their highest concentration c was at or slightly above c^*, the overlap concentration, where c^* is taken as $c[\eta] \approx 1$.

The ambient viscosities of the systems studied were measured on a Contraves low-shear 30 viscometer operating at a temperature of 22.5 ± 0.1 °C and a shear rate range of 0.0222–0.352 and 0.0758–1.20 s^{-1} for organic and aqueous solvents, respectively. The viscosities did not vary upon changing shear rate, indicating the measurements were made in the Newtonian plateau. These results are given in Table II. The shear rate in the diamond-anvil cell viscometer is not quantitatively known. It is determined by the ratio of the ball velocity (which varies with viscosity) and the gap between the diamond and the ball (which is unknown). However, we estimate the shear for the lowest viscosities (highest ball velocities) to be on the order of hundreds of reciprocal seconds and such values are consistent with previous measurements.[43]

Table I
Physical Properties of Solvents

physical properties of solvents[a]	water	THF	$CHCl_3$
dielectric constant[49]	78.54	7.26	4.81
equilibrium freezing pressure (kbar)	9.2[45]	14.2	5.2
compression at freezing pressure (%)	81.2[39,40]	71.9[41]	81.6[42]
ambient pressure viscosity (cP)	1.00	0.48	0.57
viscosity at freezing pressure (cP)	1.82	31.07	4.03
Birch–Murnaghan eq of state K_0 (kbar)[38]	21.0	10.8	8.39
Birch–Murnaghan eq of state K_0' (unitless)	7.5	9.7	13.34

[a] All values cited were determined at 22.5 ± 1 °C.

Table II
Intrinsic Viscosity and Huggins Coefficients Calculated at High and Ambient Pressures[a]

	high pressure results		ambient pressure results	
substance	$[\eta]$, dL/g	k_H	$[\eta]$, dL/g	k_H
PS/THF	1.31 ± 0.10	0.46 ± 0.11	1.34 ± 0.08	0.26 ± 0.08
PS/$CHCl_3$	1.39 ± 0.10	0.25 ± 0.08	1.32 ± 0.14	0.34 ± 0.16
PIB/THF	0.74 ± 0.07	0.36 ± 0.15	0.72 ± 0.04	0.31 ± 0.09
HPAM/2% NaCl	11.9 ± 1.1	0.83 ± 0.10	12.4 ± 0.5	0.48 ± 0.04

[a] All values cited were determined at 22.5 ± 1 °C.

Results and Discussion

For the organic polymer solutions, the pressure derivative of viscosity is dominated by the pressure depend-

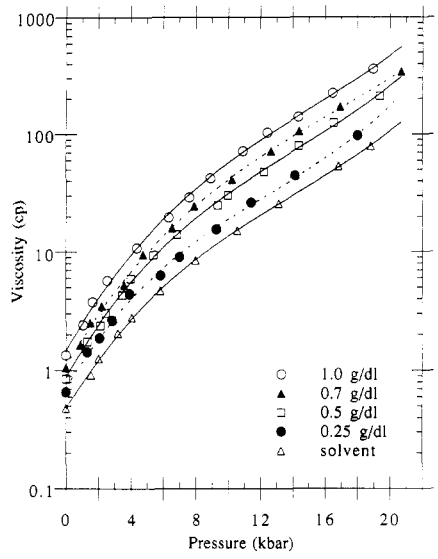

Figure 2. Viscosity–pressure relationship for PS solutions in THF. The approximately exponential dependence of viscosity on pressure for THF (bottom curve) is typical simple fluid behavior. The polymer viscosity rises faster with pressure than the solvent as discussed in the text.

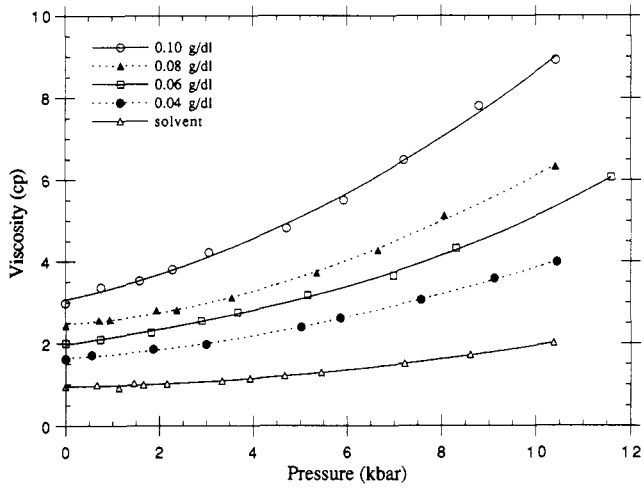

Figure 3. Viscosity–pressure relationship for HPAM in 2% NaCl solution. Note that the exponential rise in viscosity with pressure seen in organic solvents is not present for aqueous solvents. The rise in viscosity with pressure in the upper curves is due almost entirely to the polymer.

ence of the solvent viscosity. Figure 2 shows the viscosity–pressure curve for a typical system, i.e., PS in THF. For most simple liquids the viscosity rises approximately exponentially with pressure.[44] This is true for THF as well as chloroform as can be seen in the bottom curve (THF) of Figure 2. The polymer solutions (the upper curves of Figure 2) have an enhanced viscosity as compared to the solvent at zero pressure. Note that the polymer solution curves are offset and diverge slightly from the solvent curve, i.e., the distance between the curves is greater at high pressure than at low pressure. The experimental error of these data is approximately the size of the data points, and the lines drawn through them are empirical fits used for interpolation when applicable. The polystyrene (PS) in chloroform and polyisobutylene (PIB) in THF yield similar η vs P curves.

Water does not show an exponential increase in viscosity with pressure (Figure 3) as seen in the organic solvents. A possible explanation for the lower value of $d\eta/dP$ is that hydrogen bonding between water molecules is disrupted with increasing pressure. (In fact, the viscosity of water actually decreases with increasing pressure when measured at temperatures below 10 °C).[44] Indeed, water increases in viscosity by only a factor of 2 from ambient pressure to the onset of crystallization to Ice VI at 9.22 kbar and 22.5 °C.[45] As noted previously, the solvent used in this experiment is a 2% NaCl solution in water stabilized with 50 ppm formaldehyde. The addition of the salt and stabilizer was found not to change the high-pressure viscosity curve (as plotted in Figure 3) from the previously established curve of pure water.[44] This relative insensitivity of the viscosity of water to pressure allows the use of a linear rather than a semilog plot and removes the solvent dominance of the viscosity at high pressure. Therefore, the increase in viscosity observed for the HPAM solutions in Figure 3 comes almost entirely from the effect of the polymer rather than from the solvent.

In order to understand the effect of pressure upon the configuration of dissolved polymers, we calculated the specific viscosity as a function of pressure

$$\eta_{sp} = \eta/\eta_0 - 1 \tag{3}$$

where η_{sp} = specific viscosity, η = polymer solution viscosity, and η_0 = solvent viscosity. This was accomplished by taking the ratio of the viscosity of the polymer solution at the pressure of each data point to the interpolated viscosity of the solvent at the given pressure. This ratio effectively removes the solvent-dominated exponential viscosity rise as seen in Figure 2 and allows for a direct examination of polymer behavior. This is also the first step to obtaining the intrinsic viscosity from which dilute solution polymer theory can be applied

$$[\eta] \equiv \lim_{c \to 0} (\eta_{sp}/c) \tag{4}$$

where $[\eta]$ = intrinsic viscosity and c = concentration (mass/volume). $[\eta]$ is calculated from η_{sp} by the familiar Huggins equation

$$\eta_{sp} = [\eta]c + k_H[\eta]^2c^2 + \ldots \tag{5}$$

where k_H is the Huggins interaction parameter. The dilute solution theory of Flory relates the intrinsic viscosity to the radius of gyration and molecular weight through the use of eq 1.[1] Thus the behavior of η_{sp} at high pressure leads to a knowledge of the effect of pressure on the radius of gyration. This parameter is intimately connected with understanding how pressure affects a polymer's configuration.

Concentration is expressed as mass/volume in the Huggins equation (eq 5). At high pressure, the difference between mass/volume and mass/mass concentration becomes important as the volume decreases during compression. If we are to use mass/volume concentration, the concentration must be corrected to account for density changes upon compression. Figure 4 shows the consequences of this correction for PS in THF plotted in the form of a traditional Huggins plot; the reduced viscosity, $\eta_{red} = \eta_{sp}/c$, is plotted against concentration and the y-intercept is $[\eta]$. For the purpose of illustration, values of η_{red} taken at two different pressures are shown corrected (open symbols) and uncorrected (solid symbols) for concentration changes. The ambient-pressure data (solid circles) are unaffected by the concentration correction; a heavy solid line is drawn through these points. It is clear that before application of the correction, the high-pressure data differ significantly from the ambient data and from one another. Thus, using uncorrected (mass/mass) concentrations leads to a calculation of $[\eta]$ such that $[\eta]$ increases with increasing pressure (i.e., dashed lines). This

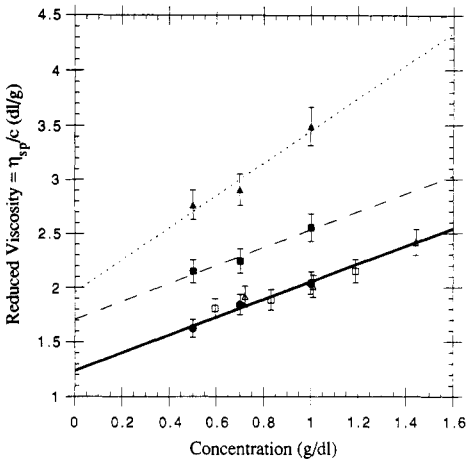

Figure 4. Huggins plot for PS in THF showing how the concentration correction affects $[\eta]$ calculation. The solid symbols are uncorrected (i.e., mass/mass concentration) and the open symbols are corrected (i.e., mass/volume concentration). The circles, squares, and triangles are at 0, 4, and 18 kbar, respectively. Note that uncorrected data give an $[\eta]$ that increases with pressure (dashed lines). The same data, once corrected, falls on the ambient-pressure (solid) line (see text).

is the method of calculation used by some previous workers.[14-16,21-23] However, when the corrected (mass/volume) concentration is used, the data collapse onto the ambient line and $[\eta]$ is constant to within experimental error; i.e., $[\eta]$ is pressure invariant. This clearly shows the importance of applying the concentration correction. This correction is very similar to that of Freeman et al.[32] except that we have neglected the polymer partial specific volume terms (see their eq 17) which is unimportant for our solutions. Significantly, applying the correction to the dynamic light scattering data on PS in toluene[32] led the authors to the conclusion that R_h is invariant with pressure. This is consistent with our conclusion that $[\eta]$ is invariant with pressure. Therefore, in order to use the Huggins equation to extract $[\eta]$ from high-pressure polymer viscosity data, one should use corrected rather than uncorrected concentrations. The collapse of η_{red} onto the ambient-pressure data implies that η_{sp} is a function of concentration only (pressure independent) as is seen in all four systems studied (see Figure 5). Remarkably, this relationship is applicable to over a 3 order of magnitude change in the base viscosity of the solvent.

Figure 5a shows a plot of η_{sp} vs concentration for PS in THF. The difference between these data and a conventional plot of this sort is that the data are obtained at pressures between 0.001 and 20 kbar. The concentration identifying each solution in the legend is the initial concentration before compression where each plot symbol represents a different PS solution whose initial concentration was set in the usual manner by dissolving a differing weight of the polymer into a specific volume of solution. As the pressure is elevated, concentration increases (as per the correction discussed above) due to increasing density; thus, the leftmost point within a set of identical plot symbols is the η_{sp} at ambient pressure for that solution. Moving to the right within a set corresponds to increasing the pressure to a maximum of about 20 kbar at the right end. The leftmost data point from each set was taken from a Contraves low-shear 30 viscometer. The results show that a single smooth curve can be drawn through all the data points. Note, for example, that the high-pressure points from the 0.5 g/dL sample overlap the low-pressure points from the 0.7 g/dL sample. The remarkable fact from this analysis is that the change in η_{sp} resulting from a change in concentration induced by increased pressure is the same as the change in η_{sp} induced by physically adding more polymer.

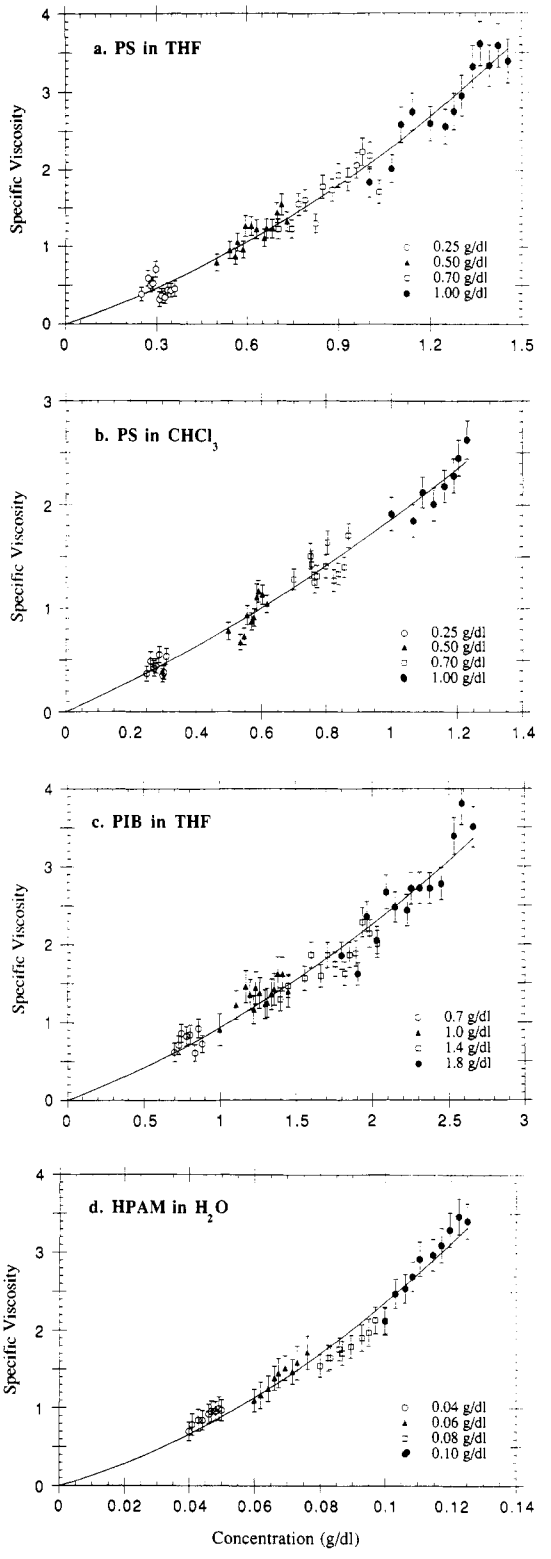

Figure 5. Specific viscosity vs concentration. The symbols in the legend represent ambient concentration. The leftmost datum within a group was taken at ambient pressure while pressure was increased to the maximum obtainable (≈20 kbar, THF; ≈6 kbar, $CHCl_3$; ≈10 kbar, H_2O) for the rightmost datum. Concentration increases with P; the data show that η_{sp} reflects this concentration change but is otherwise unaffected by pressure. This shows that, under many different conditions, $[\eta]$ is invariant with pressure. The curve is the best fit to the Huggins equation (eq 5). (a) PS in THF: $[\eta] = 1.31 \pm 0.10$ dL/g, $k_H = 0.46 \pm 0.11$. (b) PS in $CHCl_3$: $[\eta] = 1.39 \pm 0.10$ dL/g, $k_H = 0.25 \pm 0.08$. (c) PIB in THF: $[\eta] = 0.74 \pm 0.07$ dL/g, $k_H = 0.36 \pm 0.15$. (d) HPAM in 2% NaCl solution: $[\eta] = 11.9 \pm 1.1$ dL/g, $k_H = 0.83 \pm 0.10$.

The curves drawn through the data in Figure 5 represent the best fit to the Huggins equation where $[\eta]$ and k_H are fit parameters. Table II lists the values of $[\eta]$ and k_H obtained from these $[\eta]$–concentration plots at high pressure and those obtained in the Contraves viscometer at ambient pressure. The differences between the high and ambient pressure $[\eta]$ are within experimental error of our measurements. It is concluded that $[\eta]$ is invariant with pressure for this system. It should be noted that the highest concentration used is above c^* (this was done because the use of concentrations lower than 0.25 g/dL would result in propagated errors larger than the trend in the data). This causes the data to diverge slightly from what one would expect from a quadratic truncation of the Huggins equation and contributes to the fact that the k_H calculated from the high-pressure data is larger than k_H at ambient pressure (Table II). Within the resolution of our data, we can say nothing more quantitative about the variation in k_H.

In selecting other polymer–solvent systems for study, a wide variety of polymers (thermoplastic (PS) and elastomer (PIB)) and solvents (aqueous and organic) were chosen to test the scope of this invariance of $[\eta]$ with pressure. All of the systems studied were linear chains dissolved in good solvents. As noted previously, the samples were monodisperse with the exception of HPAM.

Figure 5b shows the results for PS dissolved in chloroform. The equilibrium freezing point of chloroform is 5.2 kbar at 22.5 °C which limits the pressure range spanned, and therefore the compressibility is limited to approximately 82% of the initial volume (see Table I). As a result one data set does not overlap another in Figure 5b as observed elsewhere in Figure 5. However, $[\eta]$ is still observed to be pressure invariant, as evidenced by the η_{sp} vs concentration plot and the values in Table II.

Figure 5c shows an elastomer (PIB) in THF. One reason for selecting PIB is that its backbone is more flexible than that of PS, and, consequently, one might expect any response to pressurization to be easily observed. The molecular weight of PIB was selected to have approximately the same degree of polymerization as PS. In this case the concentrations chosen are higher than those for PS in order to obtain the same range of η_{sp}; i.e., PIB has a lower $[\eta]$ than PS (Table II). Once again, PIB in THF shows that $[\eta]$ is invariant with pressure.

Figure 5d shows HPAM in 2% NaCl solution. In this case the conditions are admittedly much more complicated than the systems described above. The polyacrylamide is partially hydrolyzed which leads to the formation of carboxyl anions on the polymer chain. In dilute solution, the counterions can disassociate, causing chain expansion due to charge–charge repulsions. This polyelectrolyte effect, however, can be screened through the addition of a soluble, low molecular weight salt such as sodium chloride.[46-48] If this repulsion were present, it would lead to enhanced η_{sp} as the concentration approaches zero. The fact that η_{sp} converges toward $[\eta]$ on a plot of η_{sp}/c vs c with c as low as 0.02 g/dL indicates that the screening from the added salt ions completely shields the carboxyl group interactions. The extensive hydrogen bonding of water (which causes its unusual high-pressure viscosity behavior) is an additional complication. In spite of all these potential complications, plotting η_{sp} vs c still results in a single curve, indicating that $[\eta]$ is again invariant with pressure.

Our findings can be generalized in the equation for the high-pressure viscosity of a dilute polymer solution

$$\eta(P) = \eta_0(P)\{1 + [\eta]c(P) + k_H[\eta]^2c(P)^2\} \quad (6)$$

or recast in a simpler Huggins-like form in terms of the specific viscosity

$$\eta_{sp}(P) = [\eta]c(P) + k_H[\eta]^2c(P)^2 \quad (7)$$

Equation 6 states that the viscosity of a dilute polymer solution at any given pressure, $\eta(P)$, is equal to the right-hand side of eq 6, where $\eta_0(P)$ is the solvent viscosity at pressure P, $[\eta]$ and k_H are the Huggins equation constants (determined at ambient pressure), and $c(P)$ is the concentration corrected for fluid compression. This last term is defined through the relationship $c(P) = c(0)\,\rho(P)/\rho(0)$, where $c(0)$ is the ambient-pressure polymer concentration (in units of mass/volume) and $\rho(0)$ is the ambient fluid density. In this work $\rho(P)$, the high-pressure density, is calculated from the Birch–Murnaghan equation of state, but it could also be calculated from other equations of state or directly measured. Equation 7 gives a similar result in terms of the specific viscosity; see eq 3.

As stated earlier, all of the literature values of $[\eta]$ increase with increasing pressure. The data of Schott, Will, and Wolf[24] for poly(decyl methacrylate) in isooctane (M_w = 250 000, M_w/M_n = 1.14, T = 100 °C) and of Schmidt and Wolf for PS in *tert*-butyl acetate (M_w = 110 000, M_w/M_n = 1.06, T = 80.2 °C)[20] already contain the concentration correction used in this paper. Unlike the pressure-independent $[\eta]$ values found in our study, these two studies show $[\eta]$ initially increases upon application of pressure and then levels off between 2 and 3.5 kbar, giving a total increase of 20–25%. When the concentration correction is applied to other data, it reduces but does not eliminate the increase in $[\eta]$. This accounts for $\approx 1/3$ of the rise of $[\eta]$ with pressure for PS in benzene (M_w = 440 000) to 0.3 kbar,[22] for poly(dimethylsiloxane) in cyclohexyl bromide (M_w = 300 000) to 0.4 kbar,[16] and for PS in toluene (M_w = 209 000) to 1.0 kbar.[21] Thus the application of this correction does not always result in $[\eta]$ being pressure independent, as indeed one would expect given the variations in R_g and A_2 reported in the literature.

Clearly, for the four systems measured here, $[\eta]$ is constant to within 10% with increasing pressure, and we can now use our viscosity data to infer the molecular configuration at high pressure. We may rule out several effects of pressure that would complicate the application of eq 1 to interpret high pressure $[\eta]$ in terms of $\langle s^2\rangle^{1/2}$. There are no associating groups on any of the polymers that could link up with other polymers to form chains with a larger effective molecular weight. Also, the chains are not degraded under pressure as evidenced by the fact that viscosity measurements were made for both increasing and decreasing pressure and that the ambient-pressure viscosity was in all cases completely recovered after release from high pressure. While eq 1 was developed as a theory for use under Θ conditions, it is often applied to good solvents. For one of our systems, we have direct experimental evidence that eq 1 is applicable over a wide range of conditions. Fetters has shown that, for PS in THF, Φ' and the exponents of R_g and R_h are within 1% of their theoretical values.[43] Given the wide applicability in various solvents and polymers, it seems reasonable to apply eq 1 to the high-pressure viscosity data and conclude from the pressure invariance of $[\eta]$ that the radius of gyration is invariant with pressure.

We can use thermodynamic relationships to see what effect the invariance of the radius of gyration can reveal

about solution properties. One can use any one of several theories to see that A_2 is directly related to the radius of gyration. For example, the original Flory–Krigbaum–Orofino theory gives[27]

$$A_2 = \frac{4\pi^{2/3}N_a}{M^2}\langle R^2\rangle(P)^{3/2}0.435 \ln\left(1 + 0.885\left[\frac{\langle R^2\rangle(P)}{\langle R_0^2\rangle} - 1\right]\right) \quad (8)$$

where $\langle R^2\rangle(P)$ = high-pressure R_g, $\langle R_0^2\rangle = R_g$ of the unperturbed polymer coil, N_a = Avogadro's number, and M = polymer molecular weight. We can now obtain the thermodynamic relationship for the pressure derivative of A_2. Following the notation of Kubota et al.,[8] the thermodynamic definition of the second virial coefficient is

$$A_2 = -\Delta\mu^E/RTc^2V \quad (9)$$

where $\Delta\mu^E$ = excess chemical potential of the solvent (that in excess of an ideal solution), R = gas constant, T = temperature, c = concentration, and V = molar volume of the solvent. Taking the pressure derivative, one obtains

$$\Delta V^E/V = c^2RT[-(\partial A_2/\partial P)_T - \beta A_2] \quad (10)$$

where ΔV^E = the relative molar excess volume and β = isothermal compressibility of the solvent. Because the second term, βA_2, is typically much smaller than the first, one can see that ΔV^E controls the sign and magnitude of the change of A_2 (and related quantities). The invariance of $[\eta]$ with pressure found above indicates that ΔV^E is ≈ 0 and therefore that ideal solution behavior for the volume of mixing predominates. Clearly, ΔV^E is not always zero. One example from above is poly(dimethylsiloxane) in cyclohexyl bromide for which $\Delta V^E < 0$. As expected, $[\eta]$ for that system increases with pressure even after the concentration correction is applied.[8,16]

In light of our conclusions regarding the constancy of the radius of gyration for the four solutions studied here, it is instructive to reexamine the high-pressure data from the literature. For PS in THF there have been no other high-pressure studies, but PS has been measured in several other good solvents including one of those used here, chloroform. For PS in chloroform, A_2 has been measured up to a maximum pressure of 4 kbar and has been found to be essentially constant.[7,30] For PS in 2-butanone, both A_2 and R_g have been found to increase with pressure.[26] For PS in ethyl acetate, A_2 initially increases by a few percent but then becomes pressure independent above 2 kbar. For PS in toluene, as previously discussed (see Introduction), $[\eta]$, R_g, R_h, and A_2 have all been measured but the results are not mutually consistent. However, agreement is found between the pressure independence of A_2, measured in two different studies,[7,30] and the pressure independence of R_h, also measured in two different studies.[31,32] This is consistent with our finding that $[\eta]$ is pressure independent for PS in a good solvent. For PIB in THF there have been no high-pressure measurements in good solvents. There has been one measurement for polyacrylamide in water at high pressure in which both A_2 and R_g were measured up to a maximum pressure of 2 kbar.[28] A_2 exhibits a weak minimum as a function of increasing pressure but is equal to the ambient-pressure value for pressures above 1.5 kbar. R_g seems to decrease throughout the pressure range, but the variation is only 13% at the highest pressure. The sum of this data on good solvents, taken with our own findings, suggests that for good solvents polymer chain dimensions are often pressure independent.

Conclusions

Two major conclusions result from our experiments: (1) Our findings indicate that the concentration of high-pressure polymer solutions should be corrected to account for changing solvent density as a result of compression. Mass/volume is the correct dimension of concentration in analyzing the behavior of polymer solutions under pressure. Clearly when the pressure is increased, the accompanying change in the solvent volume elevates the polymer concentration of the solution. It is convenient to think of the corrected concentration as being proportional to the probability of finding a given polymer chain segment within a unit of volume; this probability increases as the density of the solution is increased. Calculations neglecting this correction explain why a number of studies in the literature show that $[\eta]$ systematically increases with pressure. A similar concentration correction has been applied in recent light scattering studies of R_h.[31,32] (2) Using this correction in the analysis of high-pressure viscosity data results in the collapse of calculated values of specific viscosity onto the curve defined at ambient pressure; i.e., η_{sp} is invariant with pressure. Application of a Huggins analysis shows that $[\eta]$ is therefore also pressure independent to within 10%. This implies that the microscopic picture of the effect of compression on a polymer chain in solution in the four systems studied is that the solvent is compressed preferentially so that the chain's radius of gyration is unaffected by pressure.

As concluded above, for polymers in good solvents the chain dimensions are often pressure independent. One can speculate that this is due to the good-solvent conditions. The polymer chains under these conditions are already expanded relative to Θ conditions, and perhaps pressure-induced changes in solvent quality are insufficient to significantly alter the chain dimensions once they reach this state. This suggests that under Θ conditions the polymer chain dimensions might be much more affected by pressure, and indeed the high-pressure derivative of A_2 near the Θ point can be quite large. To more fully understand this phenomenon, viscosity studies under Θ-solvent conditions are presently being pursued in our laboratory.

Acknowledgment. We express our appreciation to Bill Graessley, Gary Grest, Chris Herbst, Dudley Herschbach, Scott Milner, Sal Pace, and Jiasai Xu for their input, advice, and suggestions.

Supplementary Material Available: Tables containing the raw viscosity values, density, concentration, and calculated specific viscosity for each of the four systems (8 pages). Ordering information is given on any current masthead page.

References and Notes

(1) Flory, P. J. *Principles of Polymer Chemistry*; Cornell University Press: Ithaca, NY, 1953.
(2) Brandupt, J., Emmergut, E. H., Eds. *Polymer Handbook*, 2nd ed.; John Wiley and Sons, Inc.: New York, 1975.
(3) Ferry, J. D. *Viscoelastic Properties of Polymers*, 3rd ed.; John Wiley and Sons, Inc.: New York, 1980.
(4) Bohdanecky, M.; Kovar, J. *Viscosity of Polymer Solutions*; Elsevier Scientific Publishing Co.: Amsterdam, The Netherlands, 1982.
(5) Forsman, W. C., Ed. *Polymers in Solution*; Plenum Press: New York, 1986.
(6) Vinogradov, G. V.; Malkin, A. Ya. *Rheology of Polymers*; Mir Publishers: Moscow, 1980.

(7) Schulz, G. V.; Lechner, M. In *Light Scattering from Polymer Solutions*; Huglin, M. B., Ed.; Academic Press: New York, 1972; pp 503–528.
(8) Kubota, K.; Kubo, K.; Ogino, K. *Bull. Chem. Soc. Jpn.* **1976**, *49*, 2410.
(9) Bondor, P. L.; Hirasaki, G. J.; Tham, M. J. *Soc. Pet. Eng. J.* **1972**, *12*, 369.
(10) Chauveteau, G. *Adv. Chem.* **1986**, *213*, 227.
(11) Nielsen, L. E. *Mechanical Properties of Polymers and Composites*; Dekker: New York, 1974.
(12) Nielsen, L. E. *Polymer Rheology*; Dekker: New York, 1977.
(13) Cheng, H. S. In *CRC Handbook of Lubrication*; Booser, E. R., Ed.; CRC Press: Boca Raton, FL, 1984; Vol. II, p 139.
(14) Kammeyer, C. W. *Thesis: The Effect of Pressure on the Viscosity of Polymer Solutions, University of Illinois*; University Microfilms (Ann Arbor, MI), No. 10405; *Diss. Abstr.* **1956**, *16*, 881.
(15) Techakumpuch, S. *Thesis: A Method for Studying the Effect of Pressure on the Viscosity of Polymer Solutions, University of Illinois*; University Microfilms (Ann Arbor, MI), L.C. Card No. Mic 60-1698; *Diss. Abstr.* **1960**, *20*, 4547.
(16) Kubota, K.; Ogino, K. *Macromolecules* **1979**, *12*, 74.
(17) Schmidt, J. R.; Wolf, B. A. *Makromol. Chem.* **1979**, *180*, 517.
(18) Wolf, B. A.; Jend, R. *Macromolecules* **1979**, *12*, 732.
(19) Geerissen, H.; Schmidt, J. R.; Wolf, B. A. *J. Appl. Polym. Sci.* **1982**, *27*, 1277.
(20) Schmidt, J. R.; Wolf, B. A. *Macromolecules* **1982**, *15*, 1192.
(21) Claesson, S.; McAtee, J. L., Jr.; Ali, S. *J. Polym. Sci., Polym. Phys. Ed.* **1983**, *21*, 1873.
(22) Ali, S.; Uchida, Y. *Makromol. Chem., Rapid Commun.* **1984**, *5*, 547.
(23) Ogo, Y.; Yanagawa, K. *Mem. Fac. Eng., Osaka City Univ.* **1984**, *25*, 83.
(24) Schott, N.; Will, B.; Wolf, B. A. *Makromol. Chem.* **1988**, *189*, 2067.
(25) Geerissen, H.; Gernandt, F.; Wolf, B. A. *Makromol. Chem.* **1991**, *192*, 165.
(26) Gaeckle, D.; Patterson, D. *Macromolecules* **1972**, *5*, 136.
(27) Vennemann, N.; Lechner, M. D.; Oberthür, R. C. *Polymer* **1987**, *28*, 1738.
(28) Schulz, G. V.; Lechner, M. D.; Steinmeier, D. G. *Makromol. Chem., Rapid Commun.* **1981**, *2*, 421.
(29) Lechner, M. D.; Schulz, G. V.; Wolf, B. A. *J. Colloid Interface Sci.* **1972**, *39*, 462.
(30) McDonald, C. J.; Claesson, S. *Chem. Scr.* **1976**, *9*, 36.
(31) Roots, J.; Nyström, B. *Macromolecules* **1982**, *15*, 553.
(32) Freeman, B. D.; Soane, D. S.; Denn, M. M. *Macromolecules* **1990**, *23*, 245.
(33) Nyström, B.; Roots, J. *J. Chem. Phys.* **1983**, *78*, 2833.
(34) Nyström, B.; Olafsen, K.; Roots, J. *Polymer* **1991**, *32*, 904.
(35) Chu, B. *Laser Light Scattering*; Academic Press: New York, 1974.
(36) King, H. E., Jr.; Herbolzheimer, E.; Cook, R. L. *J. Appl. Phys.* **1992**, *71*, 2071.
(37) King, H. E., Jr.; Prewitt, C. T. *Rev. Sci. Instrum.* **1980**, *51*, 1037.
(38) Bass, J. D.; Liebermann, R. C.; Weidner, D. J.; Finch, S. J. *Phys. Earth Planet. Inter.* **1981**, *25*, 140.
(39) Lown, D. A.; Thrisk, H. R.; Wynne-Jones, L. *Trans. Faraday Soc.* **1970**, *60*, 51.
(40) Koster, H.; Franck, E. U. *Ber. Bunsen-Ges. Phys. Chem.* **1969**, *73*, 716.
(41) Schornack, L. G.; Eckert, C. A. *J. Phys. Chem.* **1970**, *74*, 3012.
(42) Bridgman, P. W. *Collected Experimental Papers*; Harvard University Press: Cambridge, MA, 1964; paper 167, Vol. VI, p 3915; *Proc. Am. Acad. Arts Sci.* **1949**, *77*, 129.
(43) Cook, R. L.; King, H. E., Jr.; Peiffer, D. G. *Macromolecules* **1992**, *25*, 629.
(44) Bridgman, P. W. *Collected Experimental Papers*; Harvard University Press: Cambridge, MA, 1964; paper 65, Vol. IV, p 2043; *Proc. Am. Acad. Arts Sci.* **1925**, *61*, 57.
(45) Bridgman, P. W. *Collected Experimental Papers*; Harvard University Press: Cambridge, MA, 1964; paper 7, Vol. I, p 213; *Proc. Am. Acad. Arts Sci.* **1911**, *47*, 441.
(46) Tanford, C. *Physical Chemistry of Macromolecules*; John Wiley and Sons, Inc.: New York, 1961.
(47) Rice, S. A.; Nagasawa, M. *Polyelectrolyte Solutions*; Academic Press: New York, 1961.
(48) Eisenberg, H. *Biological Macromolecules and Polyelectrolytes*; Clarendon Press: Oxford, England, 1976.
(49) Weast, R. C. *Handbook of Chemistry and Physics*, 70th ed., CRC Press Inc.: Boca Raton, FL, 1989; pp E50–E54.

Registry No. PS (homopolymer), 9003-53-6; PIB (homopolymer), 9003-27-4; THF, 109-99-9; Cl_3CH, 67-66-3; NaCl, 7647-14-5.